EUROPEAN SYNCHROTRON RADIATION FACILITY

INSTALLATION EUROPEENNE DE RAYONNEMENT SYNCHROTRON

ESRF

Experiment Report Form

The double page inside this form is to be filled in by all users or groups of users who have had access to beam time for measurements at the ESRF.

Once completed, the report should be submitted electronically to the User Office using the **Electronic Report Submission Application:**

http://193.49.43.2:8080/smis/servlet/UserUtils?start

Reports supporting requests for additional beam time

Reports can now be submitted independently of new proposals – it is necessary simply to indicate the number of the report(s) supporting a new proposal on the proposal form.

The Review Committees reserve the right to reject new proposals from groups who have not reported on the use of beam time allocated previously.

Reports on experiments relating to long term projects

Proposers awarded beam time for a long term project are required to submit an interim report at the end of each year, irrespective of the number of shifts of beam time they have used.

Published papers

All users must give proper credit to ESRF staff members and proper mention to ESRF facilities which were essential for the results described in any ensuing publication. Further, they are obliged to send to the Joint ESRF/ ILL library the complete reference and the abstract of all papers appearing in print, and resulting from the use of the ESRF.

Should you wish to make more general comments on the experiment, please note them on the User Evaluation Form, and send both the Report and the Evaluation Form to the User Office.

Deadlines for submission of Experimental Reports

- 1st March for experiments carried out up until June of the previous year;
- 1st September for experiments carried out up until January of the same year.

Instructions for preparing your Report

- fill in a separate form for each project or series of measurements.
- type your report, in English.
- include the reference number of the proposal to which the report refers.
- make sure that the text, tables and figures fit into the space available.
- if your work is published or is in press, you may prefer to paste in the abstract, and add full reference details. If the abstract is in a language other than English, please include an English translation.

ESRF	**Experiment title: Time Resolved Studies of the Lyotropic Phase Transitions of the Inverse Bicontinuous Cubic Phases**	**Experiment number**: CH-1636
Beamline: IDO2	**Date of experiment**: from: 29th April to: 2nd May	**Date of report**: 01/09/04
Shifts: 9	**Local contact(s)**: Dr. Stephanie Finet	*Received at ESRF:*

Names and affiliations of applicants (* indicates experimentalists):

Professor Richard Templer*/Professor John Seddon*/ Oscar Ces*/Xavier Mulet*/Charlotte Conn* (Dept of Chemistry, Imperial College, London), Professor Roland Winter/Julia Kraineva* (Dept of Chemistry, University of Dortmund, Germany), Dr Adam Squires* (The Cavendish Laboratory, University of Cambridge).

The aim of these experiments was to investigate transitions between various lyotropic liquid-crystalline phases formed by the monoelaidin (ME) / water system, including the nature of any intermediates formed. This is the first time pressure-jump experiments have been carried out on this lipid system, and we were able to begin to probe the mechanisms behind the L_α->Q_{II}^P+Q_{II}^D, L_β->Q_{II}^D, L_α -> Q_{II}^D, Q_{II}^D –> L_β and Q_{II}^D –> L_β+ Q_{II}^P phase transitions. Given that many cellular processes, including endo- and exocytosis, fat digestion and membrane budding, involve changes in membrane topology and that the inverse bicontinuous cubic phases may act as intermediates in these processes it is likely that the mechanism of formation of the cubic phase from a corresponding fluid lamellar has much in common with the mechanism of cell membrane fusion and fission. The results have indicated several interesting features which agree with measurements made by us during temperature-jump experiments and lend credence to our proposed new theory for membrane fusion processes. These include the decrease in lamellar lattice parameter on transforming to the cubic phase, the appearance of a broad low-angle peak immediately afterwards and the formation of an initially highly swollen cubic phase which decreases to an equilibrium value. A number of features not seen on temperature-jump experiments have also been noted, including the coexistence of the lamellar phase with highly swollen Q_{II}^P and Q_{II}^D phases, and the direct formation of the Q_{II}^D phase from the lamellar if a very large pressure-jump is employed.

$L_\alpha \rightarrow (Q_{II}^P + Q_{II}^D)$ Transition (figure 1a) Results from the pressure-jump experiments demonstrate that the L_α lattice parameter gradually decreases following the jump reaching a final value of 51.8Å before disappearing (Figure 2a) reflecting a geometrically constrained thinning of the bilayer associated with the transition to the cubic phase.

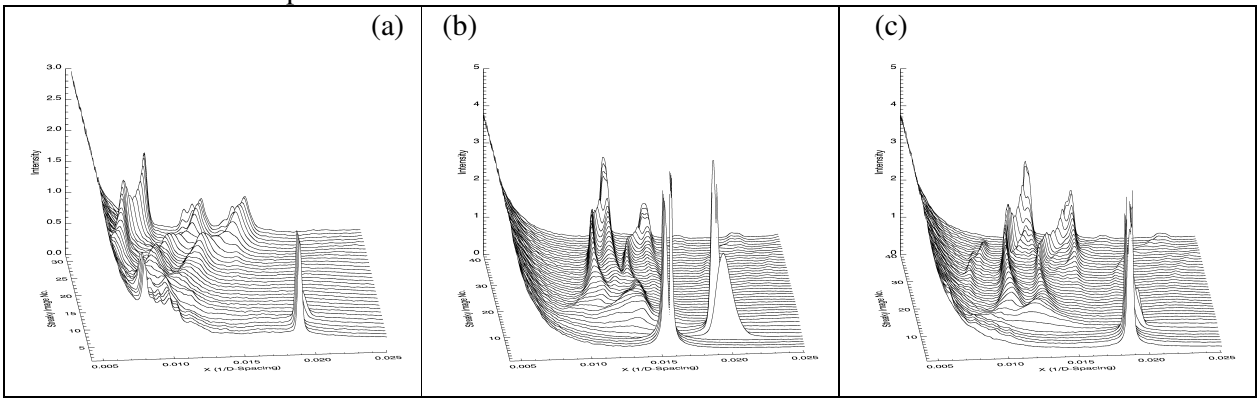

Figure 1: A series of 'stacked' plots showing transitions from the lamellar to the cubic phase. Transitions from (a) 1600-730 bar, T=59.2^{0}C (b) 1540-320 bar, T= 49.7^{0}C and (c) 1130-250 bar, T=49.6^{0}C are shown.

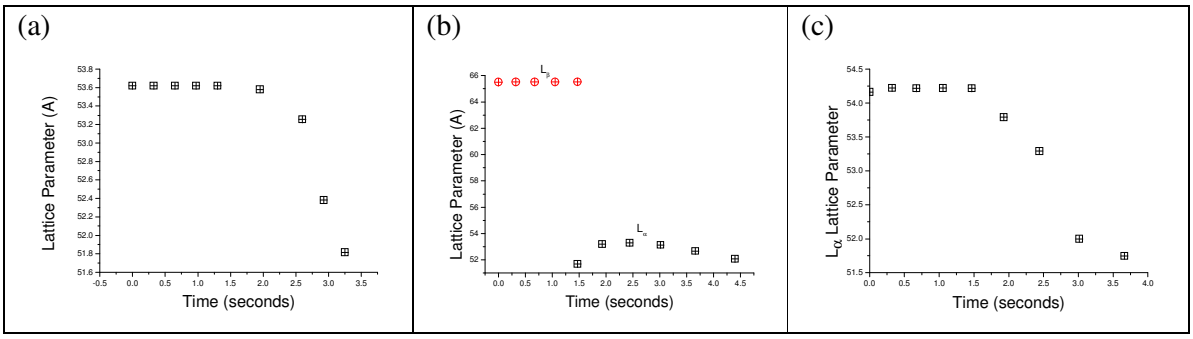

Figure 2: The decrease in L_α lattice parameter during each transition to the cubic phase. The final lattice parameter lies in a narrow band between 51.7 and 52.2Å.

This disappearance of the L_α phase is accompanied by the appearance of a broad low-angle peak from which the Q_{II}^P peaks continuously grow, which can be explained by the concerted movement of water on transforming from the lamellar to the much more highly hydrated cubic phase, resulting in a range of hydrations. This is supported by the highly swollen Q_{II}^P phase that initially forms, its lattice parameter decaying with time to an equilibrium lattice parameter of 144.5Å. The transition between the lamellar and cubic phases has been observed to pass through a highly swollen cubic phase in both the forward and reverse directions for several systems, the mechanism somehow forcing the uptake of a large amount of water by the cubic phase which is subsequently released.

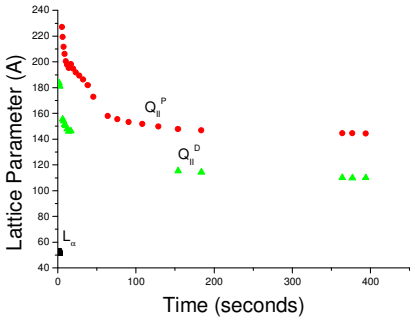

Figure 3: The evolution of lattice parameter following the transition from the L_α to the Q_{II}^P phase.

Here the initial lamellar phase coexists with several extremely swollen Q_{II}^D phases, the highest having a lattice parameter of 182.4Å. The large lattice parameter may be explained by the high pressure but the coexistence of these two phases has never before been seen under any conditions. The Q_{II}^D phase may be observed at various stages throughout the transition, its temporary absences explained by the peaks passing beneath those of the Q_{II}^P phase. The ratio of the lattice parameters of these two phases is initially high (1.41) decreasing towards an average value of 1.301. This is within 2% of a theoretical value known as the Bonnet Ratio a(P)/a(D)=1.279. A Bonnet Transformation is a mapping transformation by which the minimal surfaces upon which the cubic structures are based may be interchanged. Such a transformation, though physically unviable, gives rise to a specific ratio of lattice parameters for cubic phases coexisting under equilibrium conditions.

$L_\beta \rightarrow Q_{II}^D$ Transition Figure 1(b) shows a much larger amplitude pressure-jump beginning in the L_β phase and finishing in the Q_{II}^D cubic phase. Immediately following the jump, the lamellar phase transforms from the gel-like L_β phase to the fluid lamellar L_α. Figure 2(b) shows the layer spacing during this transition. The melting of the hydrocarbon chains causes an immediate decrease in lattice parameter due to the decrease in bilayer thickness. The broadness of the L_α peak immediately subsequent to the jump is thought to reflect a P_β intermediate phase, this cannot, however, be verified without wide-angle data. The subsequent increase in lattice parameter reflects the uptake of water due to increased bilayer repulsion in the L_α phase. We then see the gradual decrease in L_α lattice parameter associated with the transition to the cubic phase. Unlike large-amplitude temperature-jumps to the Q_{II}^D phase, the transition is not observed to pass through an intermediate

Q_{II}^{P} phase. Rather, the lamellar phase transforms directly to a swollen Q_{II}^{D} phase, again via an intermediate characterised by a broad hump in the diffraction pattern. The position of the broad hump lies to higher-angle than that noted in transitions passing though a Q_{II}^{P} phase, possibly reflecting the lower lattice parameter of the forming Q_{II}^{D} compared with the Q_{II}^{P} phase.

$L_\alpha \rightarrow Q_{II}^{D}$ Transition. Figure 1(c) shows a transition from the fluid lamellar to the Q_{II}^{D} phase, displaying several features in common with the previous transition. We again see the characteristic decrease in L_α lattice parameter (Figure 2c) before the appearance of a broad peak centred on a similar 2θ angle to that seen previously, the Q_{II}^{D} phase growing directly from this broad peak. The sharpening and intensifying of the Q_{II}^{D} peaks with time coupled with the decrease in lattice parameter towards an equilibrium value and the existence of a second Q_{II}^{D} phase decreasing to the same value are also features of both transitions. The presence of an intermediate Q_{II}^{P} phase distinguishes this transition from the previous one. Previous temperature-jump work has shown the L_α – Q_{II}^{D} transition to always proceed via an intermediate Q_{II}^{P} phase and its absence in the previous transition is unusual. However the appearance of the Q_{II}^{P} phase *after* the Q_{II}^{D} is highly unusual. The Q_{II}^{P} phase is, however, weak and initially at very low scattering angle where the noise is greatest and it is possible that the earlier peaks are simply not being detected. The four cubic phases seen throughout the transition show a marked decrease in lattice parameter with time. They may be considered as two pairs, each consisting of an Q_{II}^{P} phase and a Q_{II}^{D} phase. The lattice parameters of both sets of pairs again exhibit a ratio close to that predicted by the Bonnet relationship; one set having an average ratio of 1.275 and the second 1.286. It is interesting to note that this ratio is still upheld under the conditions above where the system is far from equilibrium.

The Inverse Bicontinuous Cubic (Q_{II}^{D}) to Lamellar (L_β) Phase Transition

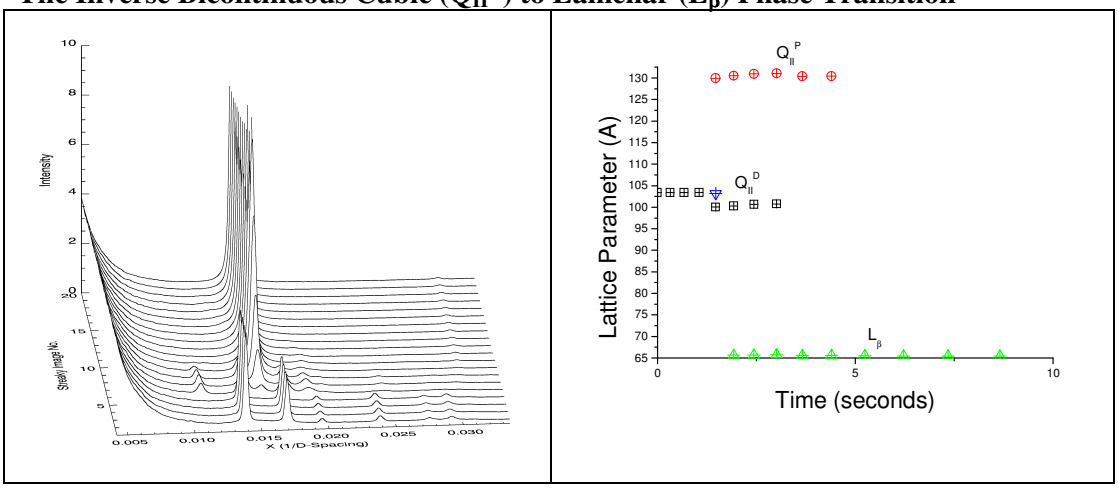

Figure 4: 'Stacked' plot showing the transitions from the cubic to the lamellar phase corresponding to a transition from 100-1650 bar, T=59.2^{0}C along with the evolution of the lattice parameter.

Pressure-jumps were employed to investigate the reverse transition from the inverse bicontinuous cubic Q_{II}^{D} phase to the lamellar phase. Figure 4 shows one such transition from 100 – 1650 bar along with the evolution of the lattice parameter of each phase The Q_{II}^{D} cubic phase passes through an intermediate Q_{II}^{P} cubic phase before exhibiting a direct transition to the gel-like L_β, bypassing the L_α phase completely.

This prelimary report has been submitted as part of our application for further beamtime at the ESRF. A more complete summary will be submitted at a later date. As demonstrated above we now have a better idea of the conditions required and timescales involved in a variety of transitions. However, a more systematic analysis is required if we are to draw firm conclusions on the mechanistic pathways and monitor effects such as that of the pressure-jump amplitude upon the kinetics. We have also measured the rate of transition as a function of the pressure-jump amplitude in order to calculate the activation energy for a variety of transitions in DOPE and MO systems, and this data is presently being analysed.